Journal of Magnetic Resonance 307 (2019) 106566

Contents lists available at ScienceDirect

Journal of Magnetic Resonance

journal homepage: www.elsevier.com/locate/jmr

One dimensional magnetic resonance microscopy with micrometer resolution in static field gradients

B. Kresse *, M.V. Höfler, A.F. Privalov, M. Vogel

Institut für Festkörperphysik, TU Darmstadt, Hochschulstr. 6, 64289 Darmstadt, Germany

ARTICLE INFO

Article history:
Received 2 May 2019
Revised 31 July 2019
Accepted 1 August 2019
Available online 3 August 2019

Keywords:
Magnetic resonance imaging (MRI)
Magnetic resonance microscopy (MRM)
Micrometer resolution
Probe head design
Static field gradient
Stray field imaging (STRAFI)

ABSTRACT

Magnetic resonance microscopy (MRM) is a valuable tool for spatially resolved studies. While it is desirable to address voxels in the general case, it is sufficient to resolve slices of the sample in many cases of practical importance, e.g., for layered structures or at planar surfaces. We demonstrate that use of high static field gradients of 73 T/m in combination with a specially designed probe head enable MRM with an ultrahigh resolution of ~2 μm in one dimension. The key feature of the built probe head is a precise computer controlled adjustment of the sample position and orientation, which allows for an accurate alignment of the samples with respect to the gradient of the magnetic field. Since slice-wise scanning of extended samples with this high spatial resolution is time-consuming, we introduce a methodology to reduce the experimental time significantly. Unlike the usual approach, which involves elaborate hardware and software correction, experimental imperfections are removed by stepwise moving the sample in our case. We demonstrate the capabilities of high-resolution 1D MRM for a solid sample with a layered structure and a liquid droplet on a planar solid substrate.

1. Introduction

The best known application of magnetic resonance imaging (MRI) is medical diagnosis in hospitals. Clinical MRI scanners have been optimized to the needs of medical applications like increasing contrasts between different tissues and reducing measuring time. While a spatial resolution of about one millimeter is usually sufficient for medical diagnosis, a higher resolution is often necessary in scientific approaches, e.g., to investigate micro-structures of biological or technological materials. Therefore, there have been considerable and successful efforts to increase the resolution towards the micrometer range [1–3], leading to the field of magnetic resonance microscopy (MRM) [4,5]. In order to reach the required gradient strength and signal-to-noise ratio, suitable small-sized pulsed field gradient (PFG) and radio frequency (RF) coils were developed. Thereby, the available space for the sample decreased to the (sub-) millimeter range [3].

For many investigations a two or three dimensional image is not required, but a one dimensional (1D) profile is sufficient. Examples include systems with layered structures or planar surfaces, which exhibit axial symmetry on the relevant length scales. To measure such 1D profiles, a gradient of the magnetic field along the symmetry axis is adequate, allowing one to employ a static field gradient (SFG). As compared to PFG approaches, SFG setups, in principle, allow one to apply stronger field gradients and, thus, to achieve higher spatial resolution. This idea was implemented using the stray field of standard superconducting magnets [6]. The method of stray field imaging (STRAFI) was further developed over the years [7–9]. Another possibility is to utilize permanent magnets, explicitly, by employing single sided magnets [10,11], a spatial resolution better than 5 μm can be achieved [12]. However, the potential of the method for high-resolution studies has not been fully exploited so far, even though there are several physical limits [13].

There are two key challenges for recording 1D profiles with high spatial resolution [14]. First, it is vital to work in a magnetic field with high gradient and planar isosurface. Second, it is necessary to well align the sample with respect to the gradient field. Here, we meet the first requirements by employing a specially designed superconducting SFG magnet, with an ultra high gradient of up to 200 T/m, which is usually used for self diffusion measurements [15] and proved useful to record one dimensional images of heavy ion irradiated crystals [16]. Moreover, we satisfy the second demand by constructing a new type of probe head, which features three computer controlled stepper motors for accurate sample positioning. In this way, we improve the spatial resolution of 1D MRM to ~2 μm and, at the same time, we benefit from a computer

* Corresponding author.
E-mail address: benjamin.kresse@physik.tu-darmstadt.de (B. Kresse).

https://doi.org/10.1016/j.jmr.2019.106566
1090-7807/

controlled automatic sample alignment, while sample positioning had to be done manually in previous approaches [14,16,17]. In addition, the probe head is constructed for various geometries of RF coils, which enables the possibility to maximize the filling factor and thereby the signal-to-noise ratio (SNR). We show that the method is applicable to liquid and solid samples, including droplets on substrates, as encountered in investigations of wetting phenomena. The present examples use ^{1}H as the probe nucleus, but the method is not limited to this case.

As a drawback, high spatial resolution comes along with long experimental times, when intending to scan extended objects. Therefore, we devise an experimental protocol that reduces the measurement time from hours to minutes. In MRI approaches to this problem, software-based corrections are usually applied to overcome experimental imperfections like non-uniform pulse excitation and resonance-circuit characteristics [18]. As an alternative, we present a method, which makes use of the possibility to move the sample along the imaging axis.

2. Theoretical background

The ^{1}H Larmor frequency is determined by the magnetic field strength, $\omega_0 = \gamma B_0$, where γ is the gyromagnetic ratio of the proton. When the magnetic field has a constant gradient G along the B_0 direction (z direction), the Larmor frequency varies in space, $\omega_0(z) = \gamma(B_0 + Gz)$, so that ω_0 of each spin is directly linked to its z coordinate. The spatial resolution Δz is determined by the gradient strength G. Specifically, for a detectable frequency shift of $\Delta\omega_0$, the spatial resolution is given by $\Delta z = \Delta\omega_0/(\gamma G)$, indicating the advantage of strong field gradients for high-resolution studies.

In our measurements, we use long, shaped RF pulses, which have a narrow frequency distribution around a center frequency ω and, hence, excite only the spins in a thin slice of the sample where the resonance condition is met, $\omega \approx \omega_0(z)$. Due to this narrow band excitation, the NMR signal decay time T_2^* is sufficiently long to record free induction decay (FID) signals. RF pulses with box-shaped excitation spectra would ensure that all excited spins are exposed to the same RF field. However, box-shaped excitation spectra require infinitely long sinc-shaped pulses, which cannot be realized experimentally. To overcome this problem, optimized pulse shapes, e.g., BURP pulses, were developed for various applications [19].

In order to record 1D images, two alternative approaches can be used. The sample can be scanned by varying either the central excitation frequency ω so that the resonance condition $\omega \approx \omega_0(z)$ is met at different slices during the scanning procedure or by moving the sample with respect to the field gradient and keeping the excitation frequency ω and, thus, the excited z range constant.

When striving for shorter measurement times, we reduce the pulse lengths so that the excitation spectrum and, thus, the excited slice become broader. Then, it is necessary to apply an echo sequence to overcome a short T_2^* due to fast dephasing of the spins. In this case, we obtain the 1D profiles from a Fourier transformation of the echo signal. Evidently, excitation of broader slices enables faster scanning. However, experimental imperfections become important when a broader frequency range is excited. Specifically, the non-rectangular shape of the excitation spectra and the non-ideal characteristic of the resonance circuit lead to distortions, which are usually corrected by software tools. An alternative method will be presented below.

3. Experimental

All experiments are performed in a custom made superconducting SFG magnet from Magnex Scientific with a bore of 54 mm. In Fig. 1(a), we show the B_0 field profile of the magnet, as calculated in previous work [20]. The maximum field strength is about 7 T just 50 mm above and below the center and thereby producing a gradient G of almost 200 T/m in the center. As aforementioned, 1D MRM studies profit from high B_0 and G values and require flat magnetic isosurfaces to enable excitation slice by slice. For the used SFG magnet, these criteria are met at positions 90 mm above or below the center of the magnet. At these positions, the field profile is planar, the field strength is 3.8 T, and the gradient strength amounts to 73 T/m, corresponding, for our case of ^{1}H, to a Larmor frequency of 160 MHz and 3.1 kHz/μm, respectively.

To move the probe head and, potentially, a cryostat, a self constructed elevator is mounted on the top of the magnet. It allows us to move all components and, thus, the sample with a nominal precision of 1 μm. The elevator consists of three stainless steel ball screws, which are driven by a stepper motor via a tooth belt and lift an aluminum plate with a bore in the middle.

For the alignment of the sample with respect to the magnetic isosurfaces a new probe head was constructed; see Fig. 1. Three computer controlled linear stepper motors (MP-20 from Physik Instrumente GmbH & Co. KG) are located outside the magnet. The typical resolution of these pushers is specified with 0.1 μm with a bidirectional repeatability of ±1 μm. They are connected to the sample holder via quartz rods, ensuring that the inaccuracy due to thermal expansion is less than 1 μm/K. With three pushers acting parallel to the gradient, the sample can be tilted around an arbitrary axis perpendicular to the field gradient as well as moved along the gradient direction. Fig. 1 also shows the sample holder and its connection to the quartz rods. The brass adapters, which are glued to the rods, have ball shaped heads with a screw thread. Springs press the sample holder onto the brass adapters so that the sample holder can slide smoothly when the sample is tilted. Various RF coil geometries can be used, depending on the sample geometry.

We investigate three samples. Two of them contain glycerol purchased from Sigma Aldrich. In one sample, glycerol fills a glass cuvette, which has rectangular cavity, in particular, a bottom,

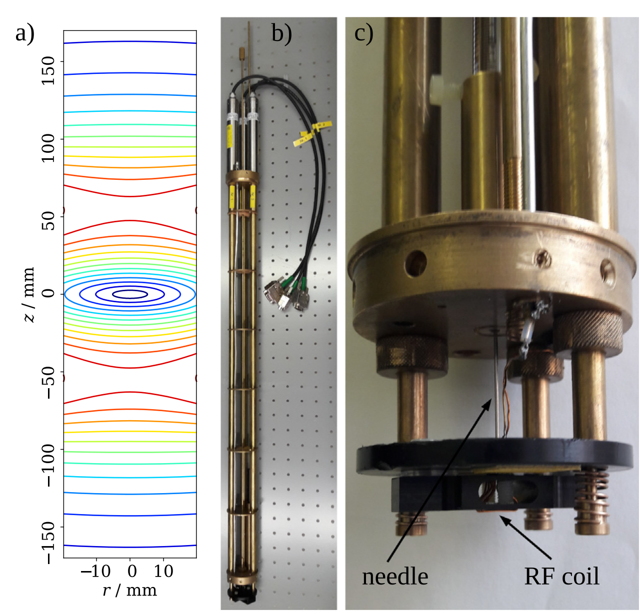

Fig. 1. (a) Magnetic field profile (isolines) of the superconducting SFG magnet [20]. (b) Probe head with three linear pusher motors for sample alignment parallel to the isolines. (c) Sample holder, which can be tilted and moved by the pushers, needle of a microliter syringe to place droplets, and RF microcoil for measurements on microliter droplets.

which is flat to a precession better than ~1 µm. In another sample, a microliter droplet of glycerol is placed on a glass substrate with a 3,3,3-Trifluoropropyl-trichlorosilane (TFPTS) modified surface, which was provided by the group of Prof. Hardt, Institute for Nano- and Microfluidics, TU Darmstadt, Germany. The third sample consists of several layers of adhesive tape glued on top of each other on a glass substrate.

For measurements of droplets at surfaces, it is necessary to deposit the liquid on the substrate while the probe head is mounted inside the magnet to avoid that it trickles down. For this purpose, a microliter syringe is mounted inside the probe head. To precisely place a droplet on the surface, we first move the substrate with the pushers close to the needle and then turn a screw, which is pushing on the plunger of the syringe. In this way, it is possible to deposit well defined microliter droplets. For the subsequent measurements of these small sample volumes, we use a solenoid RF microcoil with 5 windings to optimize the filling factor and thereby improve the SNR. The needle of the syringe can slide through the windings while placing the droplet. To avoid magnetic field distortions and short circuit of these windings due to the stainless steel needle, the coil has to be moved away from the needle for the measurement. This RF microcoil is also used for the measurements of the piled adhesive tapes.

The NMR console is controlled by the open source software DAMARIS [21,22]. The software is capable of handling serial devices like the controllers of MP-20 pushers. Moreover, DAMARIS allows us to shape RF pulses using a fast digital attenuator such as the HMC424ALP3E from Analog Devices. We apply BURP pulses [19] with a length of 1440 µs to excite sample slices of only 1 µm thickness so that FID signals can be detected. To scan the sample we either move the pushers and, thus, the sample or sweep the frequency to change the excited sample slice. In addition, we perform echo experiments using shorter pulses with lengths of a few microseconds exciting thicker slices. Due to the strong gradient of 3.1 kHz/µm, echo signals obtained from these pulses decay on the time scale of microseconds so that the width of the excited spectrum is not sufficient to address millimeter-sized samples at once. Nevertheless, echo experiments are useful to reduce the measurement times, as will be discussed in more detail below.

4. Results

First, we study a glass cuvette filled with liquid glycerol to determine the spatial resolution of our approach; see Fig. 2. The flat bottom of the cuvette with a roughness of less than 1 µm is aligned parallel to the excited slice, which has a thickness of 1 µm. For scanning, we shift the center frequency of the pulse. At each position, we measure the height of the ^{1}H FID signal, which is proportional to the number of protons in the excited slice of the sample. Thus, low and high ^{1}H FID signals are expected when the excited slice is below and above the bottom of the cuvette, respectively. The width of the step between the low- and high-signal ranges depends on both the sample alignment and the spatial resolution. Therefore, we first improve the parallel alignment of cuvette bottom and excited slice. For this purpose, we use the three stepper motors of the probe head to vary the tilting angles and systematically minimize the width of the signal rise. Fig. 2 shows the 1D MRM profile obtained after this optimization procedure. We see that the signal sharply increases within ca. 2 µm when the excited slice passes the bottom of the cuvette, while it has constant low or high values outside this region. These findings for the step width show that the achievable resolution is about 2 µm. We note that the absolute position of the step depends on the lab temperature.

Next, we test the performance of the method for a sample consisting of several layers of adhesive tape on a glass slide; see Fig. 3.

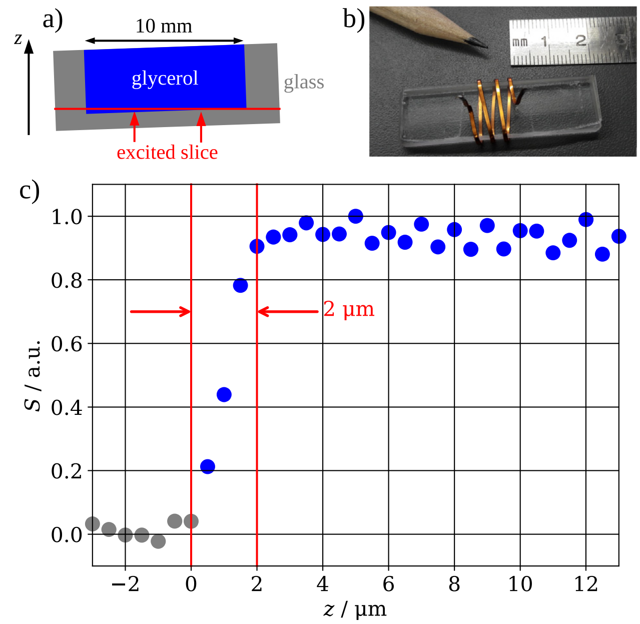

Fig. 2. 1D MRM studies of glycerol in a cuvette with flat bottom: (a) Schematic representation of a sample, which is imperfectly aligned with respect to the excited slice. (b) Picture of the sample with the used coil. The sample is covered with a glass slide. The RF coil with 3 windings is made of flat copper wire and directly wound around the cuvette. (c) Amplitude of the ^{1}H FID signal as a function of the z coordinate [dataset]. Grey and blue symbols mark sample slices through the glass substrate and the filled cavity, respectively. A spatial resolution of 2 µm is indicated by the sharpness of the step. (For interpretation of the references to color in this figure legend, the reader is referred to the web version of this article.)

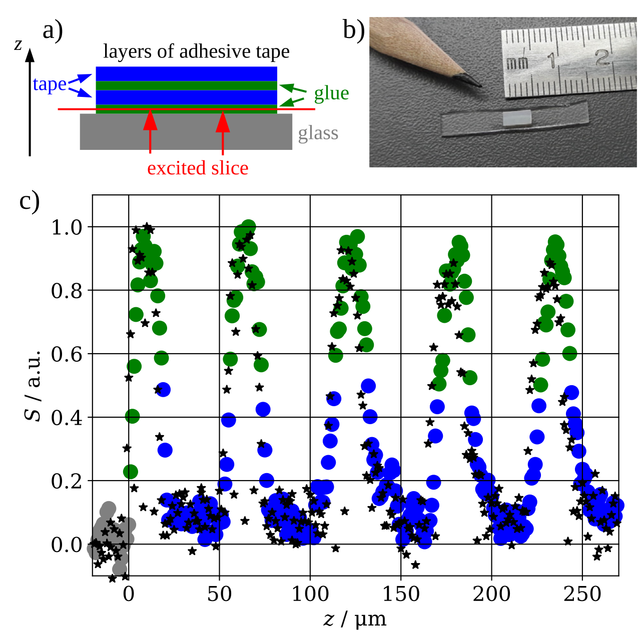

Fig. 3. 1D MRM studies of several layers of adhesive tape on a glass substrate: (a) Schematic representation of layered sample and excited slice. (b) Picture of the sample. (c) Signal amplitude as function of the z coordinate [dataset]. The ^{1}H FID signal resulting from slice selective pulses is shown as black stars (measuring time 15 hours). The ^{1}H echo signal obtained with shorter pulses using a novel method described in the text is shown as gray (substrate), green (glue), and blue (tape) circles (measuring time 50 min). An echo delay of 30 µs was used. (For interpretation of the references to color in this figure legend, the reader is referred to the web version of this article.)

For this sample, long spin-lattice relaxation times of $T_1 \gtrsim 100$ ms interfere with fast scanning. Therefore, a measurement using slice-selective pulses with an excitation width of 3 µm takes about

15 hours, but it is still feasible. The obtained 1D MRM profile (black stars) shows oscillations with a period of about 50 µm, which corresponds to the thickness of a layer of adhesive tape. The layers comprise tape and glue, which are about ~30 µm and ~20 µm thick, respectively. In this case, the amplitude of the ^{1}H FID signal is not modulated by a spatial variation of the proton density, but rather different molecular dynamics in tape and glue lead to shorter spin-spin relaxation times T_2 in the former than in the latter regions and, hence, the signal decay during the long pulse is different. In other words, the 1D MRM profile is based on T_2 contrast.

To reduce the measurement times for samples with long T_1, we devise a, to our knowledge, novel 1D imaging routine. It uses a Hahn echo sequence comprising two BURP pulses to excite and refocus the spins. The pulses have the same length of 27 µs and excite a slice of a little more than 50 µm. After a selected slice was addressed, the elevator or pushers of the probe head drive 100 µm so that the next slice of the sample is left out and the one after the next is excited by the following Hahn echo sequence. This procedure is repeated until the whole sample is scanned; see Fig. 4 (run 1a). It is necessary to skip every other slice because parts of theses regions were excited by the previous echo sequence due to the non-ideal excitation spectrum. For liquids with low viscosity, like water, even two slices need to be left out due to self-diffusion of the molecules between the exited regions. After finishing the first excitation comb, the missing slices are addressed in the same way; see Fig. 4 (run 1b). Depending on the speed of the stepper motor and the T_1 of the sample, one may have to wait for some time between subsequent excitation combs to ensure full polarization of the spins in each run. At this stage, the whole sample is scanned but the contributions of various sample regions are not completely uniform because of the non-ideal shape of the excitation spectra and the frequency dependence of the resonance circuit. Usually, phase cycles and software corrections are employed to account for these experimental imperfections. We use a different approach. Instead of accumulating the echo signals for fixed comb positions, we slightly shift the positions of the scanned slices by 1 or 2 µm after each run. The situation for the fifth run is schematically depicted in Fig. 4. This shifting procedure is repeated until the excited slices would match that during the first excitation comb. In this way, every part of the sample is scanned by all measured frequencies and non-uniform excitation effects are averaged out. Thus, a smooth image is obtained without applying any software corrections.

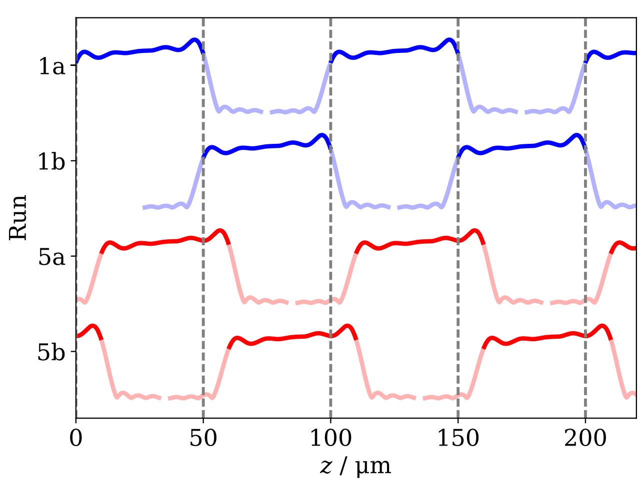

Fig. 4. Schematic representation of the used scanning protocol for echo experiments. During a scan, the sample is moved with respect to the excitation profile to obtain an excitation comb (run 1a). The skipped slices are addressed during the next scan (run 1b). Afterwards, this procedure is repeated several times with slightly shifted excitation combs each (e.g., runs 5a and 5b) to average over experimental imperfections, see text for details.

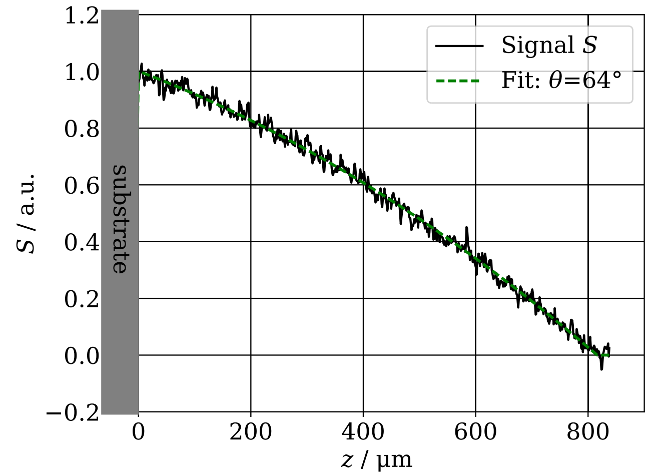

Fig. 5. 1D MRM image of a glycerol droplet with a volume of 2.5 µl on a glass substrate with a TFPTS modified surface [dataset]. The dashed line is a fit to a spherical-cap model, see Eq. (1), yielding a contact angle of 64°.

The devised scanning routine is validated for the sample consisting of piled layers of adhesive tape. In Fig. 3, we see that the results obtained from the novel procedure (circles) fully agree with that of the above described measurement (stars). For the echo experiments, the signal modulation results from different T_2 decays of tape and glue during both pulse and echo times. Using echo experiments with shorter pulses and shifting excitation combs over the sample reduces the measuring time from 15 hours for slice selective pulses to 50 min.

Finally, we apply 1D MRM to a glycerol droplet with a volume of 2.5 µl, which is placed on a glass substrate with a TFPTS modified surface. In Fig. 5, the droplet shape is evident. The 1D MRM image provides straightforward access to the droplet height, which amounts to a little more than $h = 800$ µm in the present case. The signal intensity $S(z)$ is determined by the variation of the circular slices of the droplet as a function of the distance to the substrate and is proportional to the squared radius of the slice, $S(z) \propto r^2(z)$. Specifically, the 1D profile is well described by a spherical-cap model, which gives

$$S(0 \leqslant z \leqslant h) \propto R^2 - (z-d)^2 \tag{1}$$

for a droplet sitting on a surface at $z = 0$, where R is the radius of a virtual sphere with an origin at the position d. The analysis yields a contact angle of $\Theta = 64^\circ$, in harmony with results from the groups optical measurements.

5. Conclusions

We enhanced the spatial resolution of one dimensional magnetic resonance microscopy (1D MRM) down to 2 µm. Basis for this improvement was the use of a superconducting SFG magnet with flat magnetic isosurfaces at a strong field gradient of 73 T/m. The challenge of this method is the alignment of the sample with respect to the magnetic isolines, which was achieved by construction of a probe head with three computer controlled linear stepper motors. The method was successfully validated for a liquid in a cuvette with a flat bottom, a solid with a layered structure, and a liquid droplet on a substrate. Previous manual sample alignment, by e.g. screws, can be very time consuming since two parameters (tilt angles) have to be optimized. Our computer controlled procedure significantly reduces the efforts for the experimenter, especially when performing measurements on various samples.

To reduce measurement times for high-resolution images of samples with long T_1, we devised a novel scanning protocol, which uses echo experiments with shorter pulses and shifts excitation combs over the sample so that all slices are measured with every used frequency. In this way, we overcome non-uniform excitation because we average over experimental imperfections resulting from non-ideal pulse shapes and resonance circuits, rendering use of specific phase cycles and software corrections obsolete. The method was successfully tested for a layered sample and allowed for a shortening of the measurement time by a factor of about 20.

The new setup is well suited for studies of not only layered samples but also wetting phenomena. In particular, the built probe head includes a syringe allowing us to precisely place microliter droplets on solid substrates while the probe head is inside the magnet. The achieved spatial resolution can be used to obtain position-dependent information about both structure and dynamics in future approaches. While the signal amplitudes yield spatially-resolved proton densities, measurement of T_1 and T_2 relaxation times in a slice-selective manner provides insights into spatial variations of molecular mobility.

First results show that the above described reduction of the measurement time in combination with the built-in syringe provides access to non-stationary processes, in particular, evaporation of sessile droplets. For example, concentration gradients in evaporating droplets of binary mixtures can be determined by a comparison of results for partially deuterated and non-deuterated mixtures. In particular, the proton density varies over the height of the droplet and the apparent (^{1}H NMR) contact angle might be different for those mixtures, the latter can be determined by inspecting the signal amplitude close to the substrate. Therefore a high spatial resolution and sensitivity is essential. For precise measurements on evaporating droplets and a detailed analysis of the findings, which will be the topic of a forthcoming publication, the temperature and atmosphere inside the probe need to be stabilized, which can be implemented by a constant nitrogen flow through the sample volume in the designed setup.

Data resource

Data available in data repository Dryad at http://dx.doi.org/10.25534/tudatalib-69.

Acknowledgements

We kindly acknowledge the financial support by the German Research Foundation (DFG) within the Collaborative Research Centre 1194 “Interaction between Transport and Wetting Processes”, Project A08b. We would like to thank Maximilian Hartmann and Steffen Hardt for providing us with surface modified substrates.

References

[1] J.B. Aguayo, S.J. Blackband, J. Schoeniger, M.A. Mattingly, M. Hintermann, Nuclear magnetic resonance imaging of a single cell, Nature 322 (1986) 190.
[2] R.W. Bowtell, G.D. Brown, P.M. Glover, M. McJury, P. Mansfield, Resolution of cellular structures by NMR microscopy at 11.7 T, Philos, Trans. Royal Soc. A 333 (1990) 457–467.
[3] S.-C. Lee, K. Kim, J. Kim, S. Lee, J.H. Yi, S.W. Kim, K.-S. Ha, C. Cheong, One micrometer resolution NMR microscopy, J. Magn. Reson. 150 (2001) 207–213.
[4] P.T. Callaghan, Principles of Nuclear Magnetic Resonance Microscopy, Oxford University Press, 1993.
[5] B. Blümich, W. Kuhn, Magnetic Resonance Microscopy: Methods and Applications in Materials Science, Agriculture and Biomedicine, Wiley-VCH, 1992.
[6] A.A. Samoilenko, D.Y. Artemov, L.A. Sibeldina, Formation of sensitive layer in experiments on NMR subsurface imaging of solids, JETP Lett. 47 (1988) 417–419.
[7] P. McDonald, B. Newling, Stray field magnetic resonance imaging, Rep. Prog. Phys. 61 (1998) 1441.
[8] E. Randall, Stray-Field (STRAFI) NMR: Imaging in Large Field Gradients, eMagRes, 2011.
[9] J. Mitchell, P. Blümler, P. McDonald, Spatially resolved nuclear magnetic resonance studies of planar samples, Progr. Nucl. Magn. Reson. Spectros. 48 (2006) 161–181.
[10] G. Eidmann, R. Savelsberg, P. Blümler, B. Blümich, The NMR MOUSE, a mobile universal surface explorer, J. Magn. Reson. 122 (1996) 104–109.
[11] B. Blümich, J. Perlo, F. Casanova, Mobile single-sided NMR, Progr. Nucl. Magn. Reson. Spectros. 52 (2008) 197–269.
[12] J. Perlo, F. Casanova, B. Blümich, Profiles with microscopic resolution by single-sided NMR, J. Magn. Reson. 176 (2005) 64–70.
[13] P. Glover, P. Mansfield, Limits to magnetic resonance microscopy, Rep. Prog. Phys. 65 (2002) 1489.
[14] M. Van Landeghem, B. Bresson, B. Blümich, J.-B. de Lacaillerie, Micrometer scale resolution of materials by stray-field Magnetic Resonance Imaging, J. Magn. Reson. 211 (2011) 60–66.
[15] B. Kresse, M. Hofmann, A.F. Privalov, N. Fatkullin, F. Fujara, E.A. Rössler, All polymer diffusion regimes covered by combining field-cycling and field-gradient ^{1}H NMR, Macromolecules 48 (2015) 4491–4502.
[16] M. Ditter, M. Becher, S. Orth, K. Schwartz, C. Trautmann, F. Fujara, Spatially resolved magnetic resonance studies of swift heavy ion induced defects and radiolysis products in LiF crystals, Nucl. Instrum. Methods Phys. Res. B 441 (2019) 70–78.
[17] J. Tang, G. Zhong, S. Dugar, J. Kitchen, Y. Yang, R. Fu, Solid-state STRAFI NMR probe for material imaging of quadrupolar nuclei, J. Magn. Reson. 225 (2012) 93–101.
[18] B. Belaroussi, J. Milles, S. Carme, Y.M. Zhu, H. Benoit-Cattin, Intensity non-uniformity correction in MRI: existing methods and their validation, Med. Image Anal. 10 (2006) 234–246.
[19] H. Geen, R. Freeman, Band-selective radiofrequency pulses, J. Magn. Reson. 93 (1991) 93–141.
[20] A. Gädke, Diffusionseffekte in volumenselektiver NMR auf kleinen Längenskalen (Dissertation), Technische Universität Darmstadt, 2009.
[21] A. Gädke, C. Schmitt, H. Stork, N. Nestle, DAMARIS – a flexible and open software platform for NMR spectrometer control, Diffusion Fundam. 5 (2007) 1–9.
[22] https://element.fkp.physik.tu-darmstadt.de/damaris_cms.